

Supplementary Information

Isomer Effect Study of Pyridinium-type Cationic Fluorophores: Multiple Functions and Internal Optical Mechanism

*Yasong Cao^a, Caili Zhang^b, Zhonghua Zhao^a, Haowen Huang^a, Jiatong Xu^a, Richao Shen^a, Cheng Zeng^a, Jiawei Lv^a, Ziqiang Lei^a and Hengchang Ma^{*a}*

Key Laboratory of Polymer Materials of Gansu Province, Key Laboratory of Eco-Environment-Related Polymer Materials Ministry of Education, College of Chemistry and Chemical Engineering, Northwest Normal University, Lanzhou 730070, PR China

*E-mail: mahczju@hotmail.com

Table of Contents

1. EXPERIMENTAL SECTION

2. RESULTS

3. NMR data spectra

4. HRMS data spectra

5. REFERENCES

1. EXPERIMENTAL SECTION

1.1 Materials and Chemicals.

The chemicals used in the experiments included carbon tetrachloride (CCl₄, 99%), ultra-pure water (water purifier, Resistivity of 18 mΩ*cm), Ethyl Alcohol (C₂H₅OH, 99.9%), tetrahydrofuran (THF, 99%), petroleum ether (PE, 98%), ethyl acetate (EA, 98%), dichloromethane (DCM, 99.5%), hexane (98%), methanol (C₂H₅OH, 99.9%), The materials used in the experiments included BPO (75%), Pd(pph₃)₄ (99%), Pd(OAc)₂ (99%), K₂CO₃ (99.9%), Mg₂SO₄ (99%), 4-methylbenzophenone (98%), *N*-bromosuccinimide (NBS, 99%), (4-(diphenylamino)phenyl)boronic acid (98%), 2-bromopyridine (99%), 3-bromopyridine (98%), 4-bromotriphenylamine (98%), pyridine-4-boronic acid (98%). The progress of all reactions was monitored by TLC using glass plates precoated with silica gel 60 F254 to a thickness of 0.5 mm. Silica gel (Guiyang Chanyuan Zhi-Cheng Biotechnology Co.) was used for column chromatography. All chemical materials used in this study were obtained from commercial suppliers without further purified.

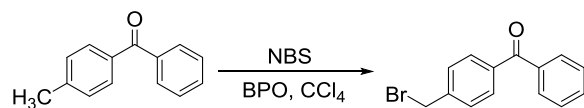
1.2 Measurements and Methods.

¹H NMR (600 MHz), ¹³C NMR (150 MHz) spectra were recorded on MERCURY spectrometer at 25 °C in CDCl₃ or DMSO-*d*₆. All chemical shifts (δ) were reported in ppm and coupling constants (J) in Hz. High resolution mass spectra (HRMS) were recorded using Thermoscientific Q

Exactive instruments under electrospray ionization (ESI) conditions. UV-visible absorption spectra (UV) were recorded on a TU-1901 and UV-3600i plus spectrometer. Fluorescence spectra were measured using a FluoroSENS 9003 fluorescence spectrophotometer at room temperature. Solid-state quantum yield was measured using a Hamamatsu C11347 Quantaurs-QY integrating sphere. Fluorescence lifetime was obtained on FluoTime 300. Optimization of molecular structures and electronic excitation calculations from S_0 to S_1 at the B3LYP/6-31G(d) computational level used the DFT and TDDFT methods to calculate in Gaussian 09 software drawing with VMD and Multiwfn. X-ray diffraction (XRD) was carried out with a Rigaku (Japan) D/max-2400 X-ray powder diffractometer, using Ni-filtered Cu $K\alpha$ radiation at 40 kV and 40 mA. X-ray crystallography was achieved using a SuperNova X-ray single crystal diffractometer with graphite monochromated Mo- $K\alpha$ radiation ($\lambda = 0.71073 \text{ \AA}$) or Cu- $K\alpha$ radiation ($\lambda = 1.54184 \text{ \AA}$).

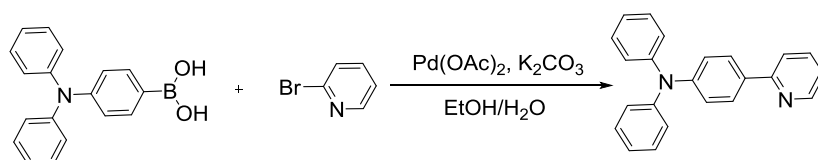
1.3 The syntheses route of molecules

1.3.1 (4-(bromomethyl)phenyl)(phenyl)methanone (BP-Me-Br)^[1]



4-Methylbenzophenone (1.96 g, 196.24 g·mol⁻¹, 10.00 mmol) and NBS (2.14 g, 177.98 g·mol⁻¹, 12.00 mmol) were placed in a 100 mL flask. Then, 30 mL of CCl₄ was added to dissolve the components. The reaction was heated to 50 °C under N₂ atmosphere; meanwhile, BPO (10.00 mg) was slowly added to the reaction solution using a balloon. Next, the reaction was refluxed under light conditions for 8 hours. Finally, the reaction mixture was concentrated by rotary evaporation and the crude product was purified by silica gel column using petroleum ether as eluent to give BP-Me-Br as white solid (yield: 93%). ¹H NMR (400 MHz, Chloroform-d) δ 7.79 (dd, J = 7.5, 4.7 Hz, 4H), 7.60 (t, J = 7.4 Hz, 1H), 7.49 (dt, J = 10.0, 5.2 Hz, 4H), 4.53 (s, 2H). ¹³C NMR (150 MHz, Chloroform-d) δ 195.96, 142.09, 137.45, 137.37, 132.56, 130.53, 130.33, 130.03, 130.00, 128.94, 128.42, 128.34, 126.55, 32.26.

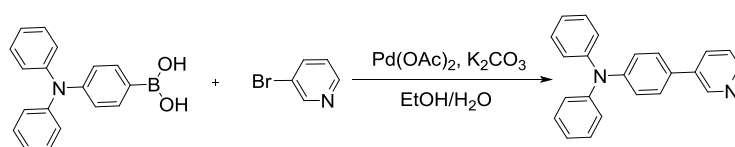
1.3.2 *N,N*-diphenyl-4-(pyridin-2-yl)aniline (*o*-TPA-Py)^[2]



(4-(diphenylamino)phenyl)boronic acid (2.60 g, 289.14 g·mol⁻¹, 9.00 mmol), 2-bromopyridine (1.00 g, 158.00 g·mol⁻¹, 6.33 mmol), Pd(OAc)₂ (20.00 mg, 224.49 g·mol⁻¹, 0.09 mmol) and K₂CO₃ (1.65 g, 138.20 g·mol⁻¹

¹, 11.94 mmol) were transferred to a 100 mL round flask. Then a mixed solvent of CH₃CH₂OH (24 mL) and H₂O (8 mL) was added and the reaction was refluxed at 80 °C for 16 hours. The organic solvent was concentrated by rotary evaporation. Next, the reaction mixture was extracted three times with DCM and H₂O, removing residual water with Mg₂SO₄. Eventually, the crude product was purified by silica gel column using a mixture (ethyl acetate/petroleum ether, 1:40) as eluent to give *o*-TPA-Py in white solid form (yield: 81%). ¹H NMR (400 MHz, Chloroform-d) δ 8.66 (d, J = 4.7 Hz, 1H), 7.87 (d, J = 8.7 Hz, 2H), 7.72 – 7.65 (m, 2H), 7.28 (t, J = 7.8 Hz, 4H), 7.15 (dd, J = 8.1, 4.4 Hz, 7H), 7.05 (t, J = 7.3 Hz, 2H). ¹³C NMR (150 MHz, Chloroform-d) δ 157.05, 149.54, 148.71, 147.47, 136.66, 133.06, 129.31, 127.73, 124.73, 123.22, 123.20, 121.45, 119.86.

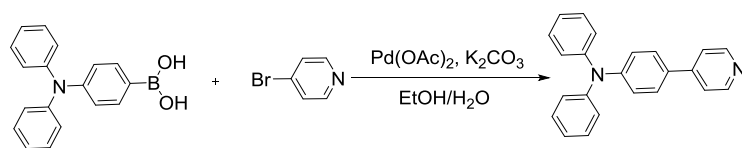
1.3.3 *N,N*-diphenyl-4-(pyridin-3-yl)aniline (*m*-TPA-Py)^[2]



(4-(diphenylamino)phenyl)boronic acid (2.60 g, 289.14 g·mol⁻¹, 9.00 mmol), 3-bromopyridine (1.00 g, 158.00 g·mol⁻¹, 6.33 mmol), Pd(OAc)₂ (20.00 mg, 224.49 g·mol⁻¹, 0.09 mmol) and K₂CO₃ (1.65 g, 138.20 g·mol⁻¹, 11.94 mmol) were transferred to a 100 mL round flask. Then a mixed solvent of CH₃CH₂OH (24 mL) and H₂O (8 mL) was added and the reaction was refluxed at 80 °C for 16 hours. The organic solvent was

concentrated by rotary evaporation. Next, the reaction mixture was extracted three times with DCM and H₂O, removing residual water with Mg₂SO₄. Eventually, the crude product was purified by silica gel column using a mixture (ethyl acetate/petroleum ether, 1:80) as eluent to give *m*-TPA-Py in white solid form (yield: 82%). ¹H NMR (600 MHz, DMSO-*d*₆) δ 8.83 (s, 1H), 8.49 (d, J = 4.3 Hz, 1H), 8.00 (d, J = 7.4 Hz, 1H), 7.63 (d, J = 8.5 Hz, 2H), 7.42 (dd, J = 7.6, 4.5 Hz, 1H), 7.31 (t, J = 7.8 Hz, 4H), 7.05 (td, J = 13.5, 12.7, 8.1 Hz, 8H). ¹³C NMR (150 MHz, Chloroform-*d*) δ 148.05, 147.80, 147.77, 147.43, 136.19, 133.83, 131.16, 129.37, 127.76, 124.71, 123.54, 123.31.

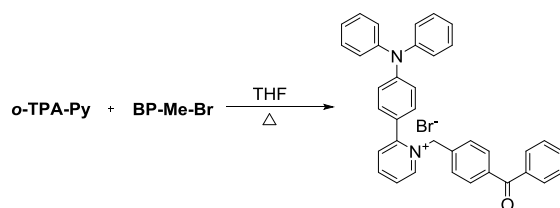
1.3.4 *N,N*-diphenyl-4-(pyridin-4-yl)aniline (*p*-TPA-Py)^[2]



(4-(diphenylamino)phenyl)boronic acid (2.60 g, 289.14 g·mol⁻¹, 8.99 mmol) and 3-bromopyridine (1.00 g, 158.00 g·mol⁻¹, 6.33 mmol), Pd(OAc)₂ (20.00 mg, 224.49 g·mol⁻¹, 0.09 mmol) and K₂CO₃ (1.65 g, 138.20 g·mol⁻¹, 11.94 mmol) were transferred to a 100 mL round-bottom flask. Then a mixed solvent of THF (25 mL) and CH₃OH (25 mL) was added and the reaction was refluxed at 80 °C under N₂ for 18 hours. The reaction mixture was concentrated by rotary evaporation and the reactants were extracted three times with DCM and water, then the residual water was removed with Mg₂SO₄. The crude product was purified on a silica gel

column with mixed solvent (ethyl acetate: petroleum ether, 1:50) as eluent and *p*-TPA-Py was obtained as a white solid (yield: 85%). ¹H NMR (400 MHz, DMSO-*d*₆) δ 8.81 (d, J = 6.5 Hz, 2H), 8.26 (d, J = 6.6 Hz, 2H), 7.95 (d, J = 8.8 Hz, 2H), 7.39 (t, J = 7.7 Hz, 4H), 7.17 (dd, J = 19.3, 7.5 Hz, 6H), 6.95 (d, J = 8.8 Hz, 2H). ¹³C NMR (150 MHz, DMSO-*d*₆) δ 154.83, 151.25, 146.24, 142.14, 130.42, 129.80, 126.35, 125.78, 125.51, 122.43, 120.40.

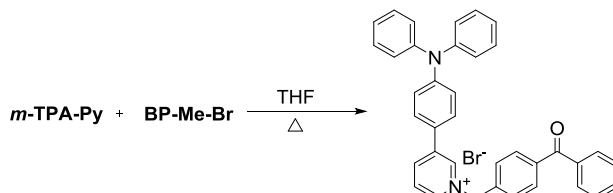
1.3.5 1-(4-benzoylbenzyl)-2-(4-(diphenylamino)phenyl)pyridin-1-ium (*o*-TPA-Pyr-BP)^[3]



o-TPA-Py (0.25 g, 322.41 g·mol⁻¹, 0.77 mmol), BP-Me-Br (0.26 g, 275.15 g·mol⁻¹, 0.97 mmol) and THF (40 mL) were added to a 100 mL round bottom flask. Then, the mixture was refluxed at 80 °C for 36 hours. Afterwards, the crude product was precipitated from THF and washed several times with THF and *n*-hexane. A green solid powder (87%) was obtained. ¹H NMR (400 MHz, DMSO-*d*₆) δ 9.41 (d, J = 6.0 Hz, 1H), 8.71 (t, J = 7.7 Hz, 1H), 8.22 (t, J = 6.4 Hz, 1H), 8.11 (d, J = 8.3 Hz, 1H), 7.65 (q, J = 10.1, 9.3 Hz, 5H), 7.51 (t, J = 7.7 Hz, 2H), 7.39 – 7.28 (m, 6H), 7.11 (dt, J = 12.9, 7.4 Hz, 8H), 6.91 (d, J = 8.7 Hz, 2H), 6.04 (s, 2H). ¹³C NMR (150 MHz, DMSO-*d*₆) δ 195.64, 155.65, 150.02, 147.50, 146.86, 146.51, 138.94, 137.20, 137.15, 133.39, 131.31, 130.86, 130.32, 130.30, 130.03, 129.07, 128.20, 127.33, 125.77, 125.03, 124.16, 120.77, 61.67. ESI⁺

HRMS m/z calcd for $C_{37}H_{29}ON_2$ 517.2257 [M].

1.3.6 1-(4-benzoylbenzyl)-3-(4-(diphenylamino)phenyl)pyridin-1-ium (*m*-TPA-Pyr-BP)^[3]

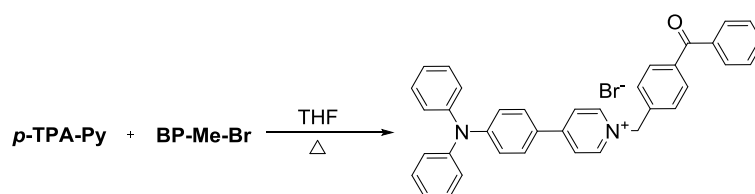


m-TPA-Py (0.25 g, 322.41 $g \cdot mol^{-1}$, 0.77 mmol), BP-Me-Br (0.26 g, 275.15 $g \cdot mol^{-1}$, 0.97 mmol) and THF (40 mL) were added to a 100 mL round-bottomed flask. Then, the mixture was refluxed at 80 °C for 36 hours. Afterwards, the crude product was precipitated from THF and washed several times with THF and *n*-hexane. A yellow solid powder (92%) was obtained. ¹H NMR (400 MHz, DMSO-*d*₆) δ 9.72 (s, 1H), 9.12 (d, $J = 6.0$ Hz, 1H), 8.93 – 8.84 (m, 1H), 8.26 – 8.17 (m, 1H), 7.83 (d, $J = 8.7$ Hz, 2H), 7.77 (s, 4H), 7.69 (dd, $J = 16.1, 7.3$ Hz, 3H), 7.54 (t, $J = 7.6$ Hz, 2H), 7.36 (t, $J = 7.9$ Hz, 4H), 7.10 (ddd, $J = 22.7, 15.0, 8.1$ Hz, 8H), 6.03 (s, 2H). ¹³C NMR (151 MHz, DMSO-*d*₆) δ 195.68, 146.78, 142.77, 142.61, 142.48, 140.14, 139.00, 138.13, 137.04, 133.44, 130.70, 130.29, 130.11, 129.31, 129.10, 128.97, 125.81, 125.56, 124.79, 122.07, 63.23, 40.52. ESI⁺ HRMS m/z calcd for $C_{37}H_{29}ON_2$ 517.2257 [M].

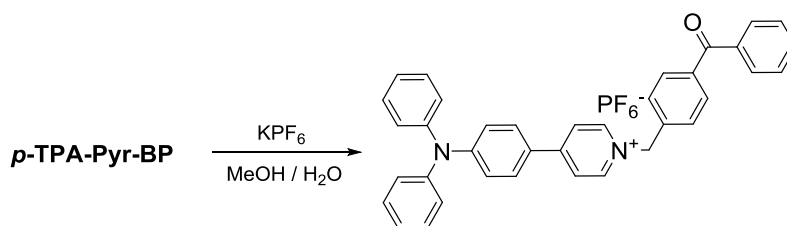
1.3.7 1-(4-benzoylbenzyl)-4-(4-(diphenylamino)phenyl)pyridin-1-ium (*p*-TPA-Pyr-BP)^[3]

p-TPA-Py (0.25 g, 322.41 $g \cdot mol^{-1}$, 0.77 mmol), BP-Me-Br (0.26 g, 275.15 $g \cdot mol^{-1}$, 0.97 mmol) and THF (40 mL) were added to a 100 mL round

bottom flask. Then, the mixture was refluxed at 80 °C for 36 hours. After that, the crude product was precipitated from THF and washed several times with THF and *n*-hexane. A green solid powder (91%) was obtained. ¹H NMR (400 MHz, DMSO-*d*₆) δ 9.12 (d, J = 7.0 Hz, 2H), 8.41 (d, J = 7.0 Hz, 2H), 8.00 (d, J = 9.0 Hz, 2H), 7.78 (d, J = 8.3 Hz, 2H), 7.70 (t, J = 7.9 Hz, 5H), 7.55 (t, J = 7.6 Hz, 2H), 7.41 (t, J = 7.8 Hz, 4H), 7.20 (dd, J = 19.0, 7.9 Hz, 6H), 6.94 (d, J = 8.9 Hz, 2H), 5.90 (s, 2H). ¹³C NMR (150 MHz, DMSO-*d*₆) δ 195.69, 154.63, 151.80, 145.99, 144.89, 139.34, 138.03, 137.07, 133.44, 130.73, 130.48, 130.20, 130.11, 129.11, 129.09, 126.62, 125.85, 123.36, 119.80, 61.78. ESI⁺ HRMS *m/z* calcd for C₃₇H₂₉ON₂ 517.2281 [M].



1.3.8 *p*-TPA-Pyr-BP/PF₆⁻[4]



p-TPA-Pyr-BP (100.00 mg, 597.12 g·mol⁻¹, 0.17 mmol) was added to a 10 mL glass vial, then 1 mL of methanol was added to dissolve it completely, after that 9 mL of ultrapure water was added to the glass vial. After the solution was homogeneously mixed, KPF₆ (36.81 mg, 184.06 g·mol⁻¹, 0.20

mmol) was added to it and it was observed under UV light that the solution instantly turned red and a reddish-brown precipitate was produced. After standing for 2 hours, the solution became clear and transparent and a reddish-brown precipitate was formed at the bottom. The crude product was washed five times with ultrapure water to obtain a reddish-brown solid (95% yield). ^1H NMR (400 MHz, $\text{DMSO-}d_6$) δ 9.06 (d, $J = 6.8$ Hz, 2H), 8.39 (d, $J = 6.7$ Hz, 2H), 7.98 (d, $J = 8.9$ Hz, 2H), 7.79 (d, $J = 8.1$ Hz, 2H), 7.69 (dd, $J = 20.4, 7.6$ Hz, 5H), 7.55 (t, $J = 7.5$ Hz, 2H), 7.42 (t, $J = 7.8$ Hz, 4H), 7.24 - 7.16 (m, 6H), 6.95 (d, $J = 8.8$ Hz, 2H), 5.85 (s, 2H). ^{13}C NMR (151 MHz, $\text{DMSO-}d_6$) δ 195.68, 154.68, 145.99, 144.88, 139.29, 138.05, 133.44, 130.75, 130.48, 130.18, 130.11, 129.11, 129.03, 126.63, 125.86, 124.58, 123.36, 119.82, 61.92. ESI⁺ HRMS m/z calcd for $\text{C}_{37}\text{H}_{29}\text{ON}_2$ 518.2280 [M].

2.RESULTS

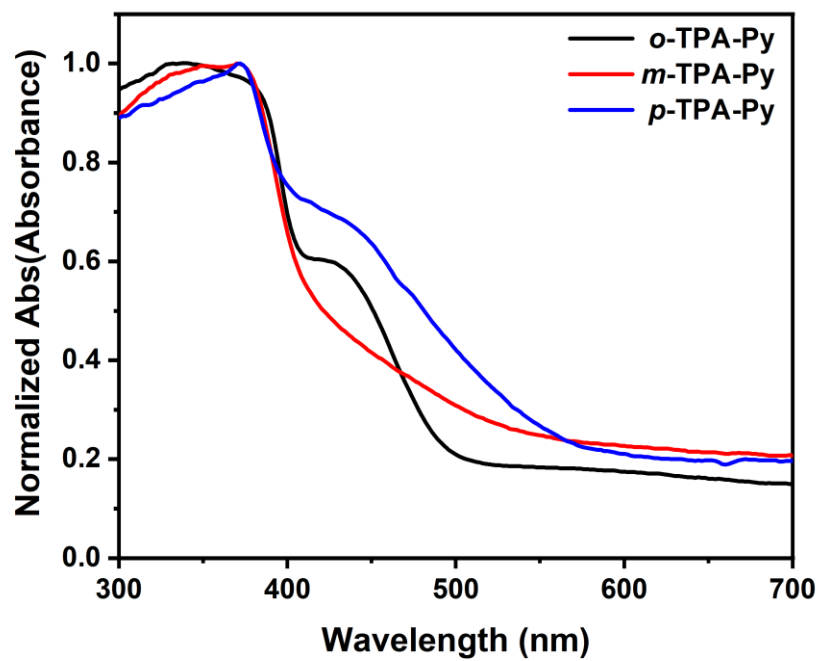


Figure. S1 The normalized solid-state absorption spectra of *o*-, *m*-, *p*-TPA-Py in solid state at 25 °C.

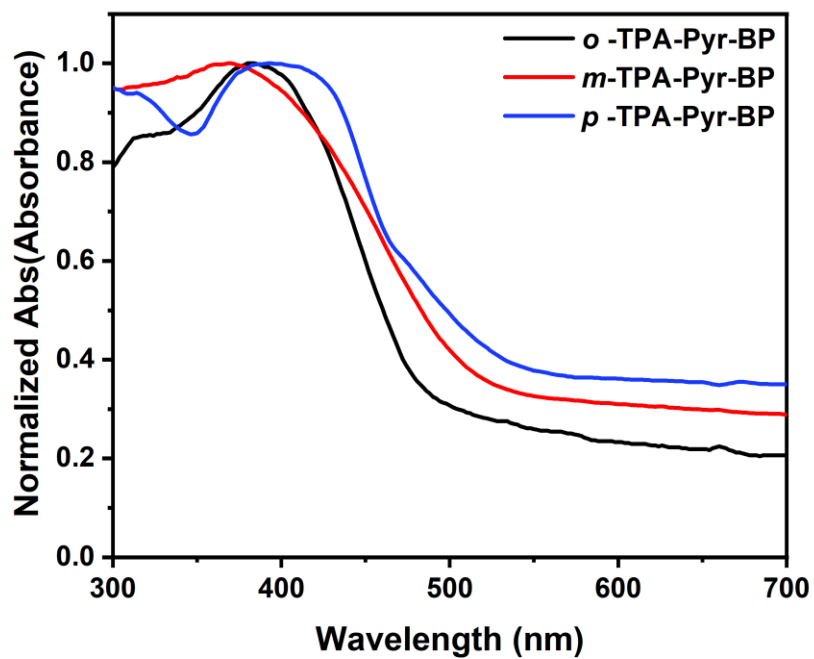


Figure. S2 The normalized solid-state absorption spectra of *o*-, *m*-, *p*-TPA-Pyr-BP in solid state at 25 °C.

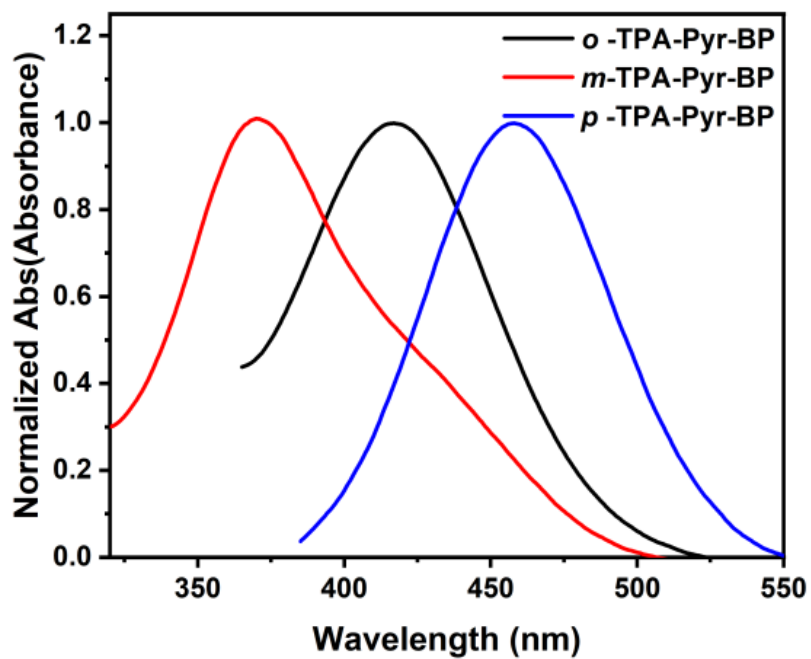


Figure. S3 Normalized absorption spectra of *o*-, *m*-, *p*-TPA-Pyr-BP in solvent of DCM (Conc. = 5 μ M) at 25 $^{\circ}$ C. (λ_{ab} = 417, 371 and 457 nm, respectively.)

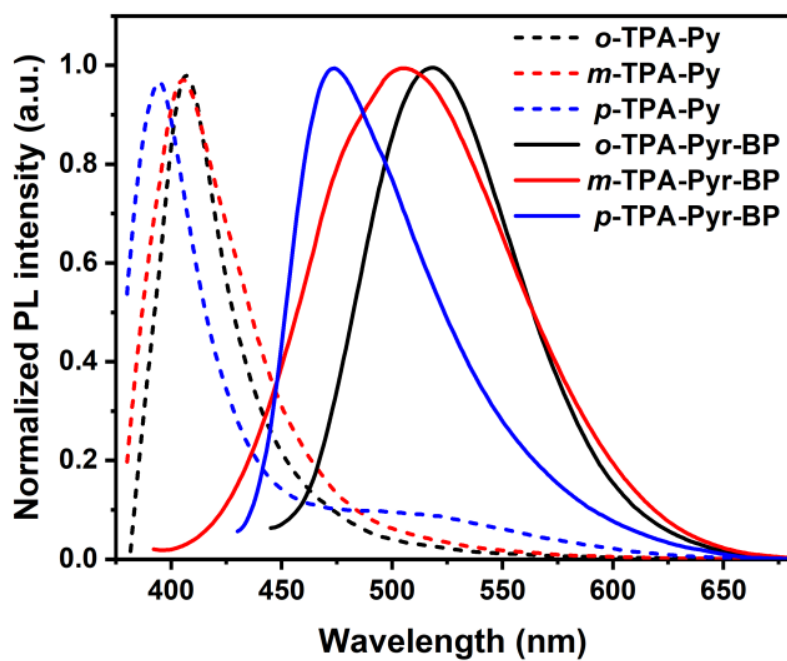


Figure. S4 Fluorescence spectra of *o*-, *m*-, *p*-TPA-Py and *o*-, *m*-, *p*-TPA-Pyr-BP in solid-state at 25 °C. (λ_{ex} = 330, 350, 350, 385 370, and 395 nm, respectively.)

Table S1. The photophysical properties and sensing capability to PF₆⁻ of *o*-, *m*- and *p*-TPA-Pyr-BP

Samples	λ_{ab} (solid state)	λ_{ab} (DCM)	λ_{em} (before grinding)	λ_{em} (after grinding)	Δ_{values}	ϕ_F	$\langle T_F \rangle$	PF ₆ ⁻ sensing capability
<i>o</i> -TPA-Pyr-BP	385 nm	417 nm	512 nm	559 nm	47 nm	68%	8.20 ns	poor
<i>m</i> -TPA-Pyr-BP	370 nm	371 nm	490 nm	566 nm	76 nm	63%	5.16 ns	average
<i>p</i> -TPA-Pyr-BP	395 nm	458 nm	479 nm	600 nm	121 nm	78%	2.97 ns	excellent

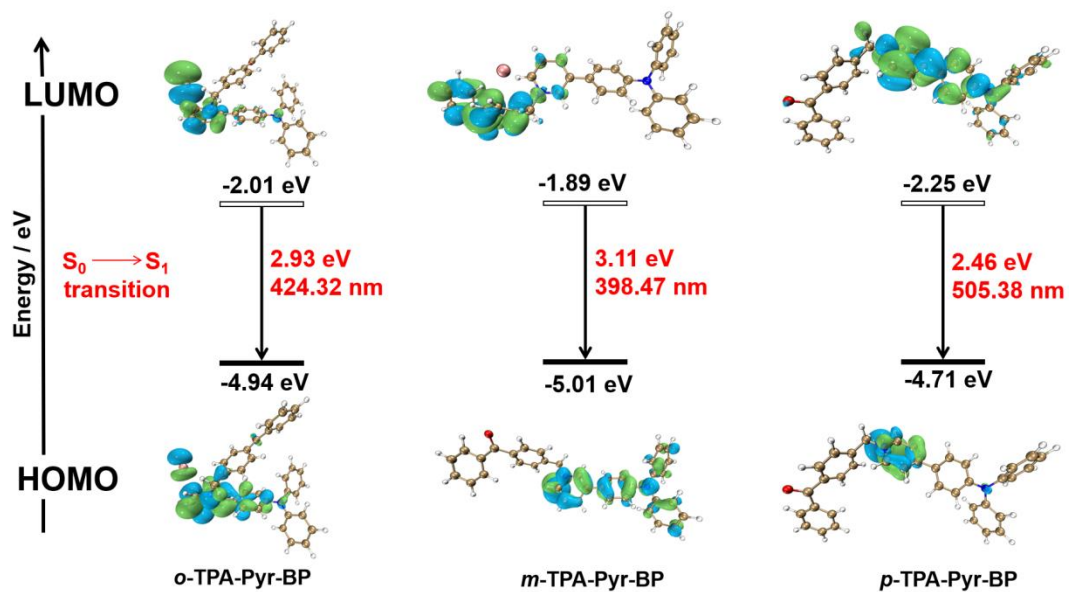


Figure. S5 Molecular orbital energy diagrams for *o*-, *m*-, *p*-TPA-Pyr-BP at B3LYP/6-31G(d) by Gaussian 09.

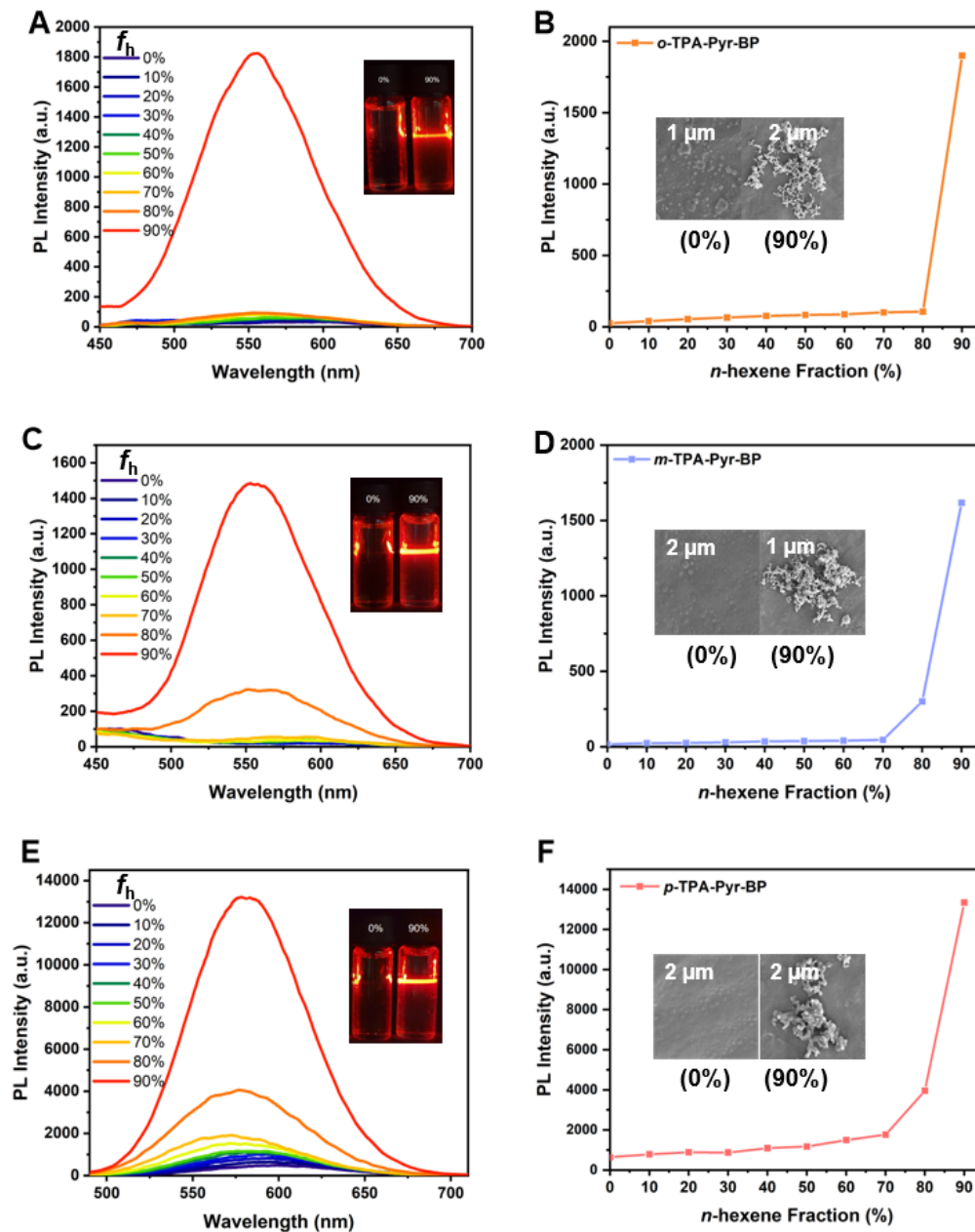


Figure. S6 PL spectra of *o*-TPA-Pyr-BP (A), *m*-TPA-Pyr-BP (B), *p*-TPA-Pyr-BP (C) (50 μM) in DCM solution with different fractions of *n*-hexane. (Inset: Tyndale effect at $f_h = 0\%$ and 90%); Fluorescence line graphs of *o*-TPA-Pyr-BP (B), *m*-TPA-Pyr-BP (D), *p*-TPA-Pyr-BP (F) at different *n*-hexane concentrations (Inset: SEM images at $f_h = 0\%$ and 90%). ($\lambda_{\text{em}} = 420, 400$ and 460 nm, respectively.)

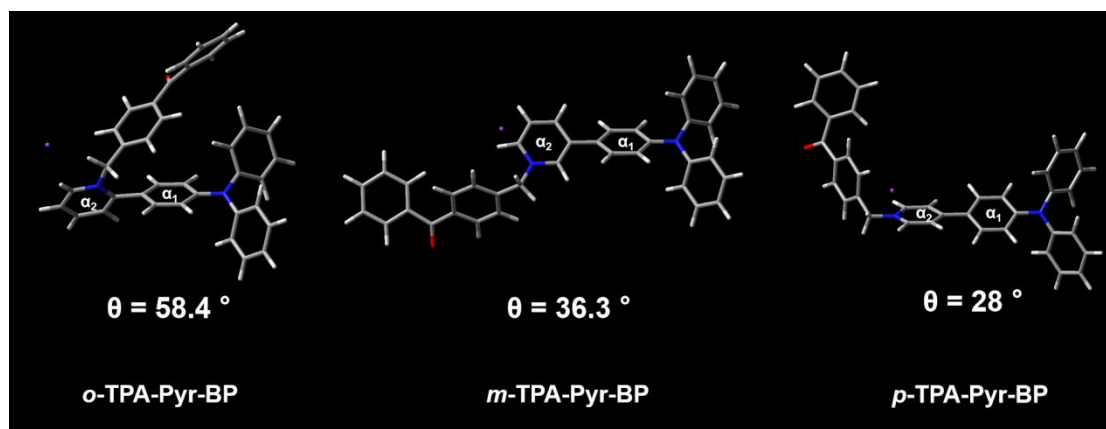


Figure. S7 The torsion angel (θ) between the benzene ring in triphenylamine (TPA) and the adjacent pyridine of *o*-, *m*-, *p*-TPA-Pyr-BP under their optimal conformation.

Table S2. Crystal data of *m*-TPA-Pyr-BP and *p*-TPA-Pyr-BP.

Name	<i>m</i> -TPA-Pyr-BP	<i>p</i> -TPA-Pyr-BP
Formula	C ₃₇ H ₂₉ N ₂ OBr·H ₂ O	C ₃₇ H ₂₉ N ₂ OBr
Wavelength(Å)	1.54184	1.54184
Space Group	P b c a	P 21/a
Cell Lengths (Å)	a 15.1563 (2)	a 9.1969 (3)
	b 9.8883 (1)	b 17.9584 (4)
	c 39.4971 (5)	c 20.7468 (6)
Cell Angles (°)	α 90	α 90
	β 90	β 100.438 (3)
	γ 90	γ 90
Cell Volume (Å ³)	5919.43 (12)	3369.91 (17)
Z	8	4
Density (g/cm ³)	1.381	1.178
F(000)	2544.0	1232.0
h _{max} , k _{max} , l _{max}	19,12,50	11,21,25
R (all data)	R ₁ = 0.0402 (5572)	R ₁ = 0.0656 (4273)
	wR ₂ = 0.1041 (6173)	wR ₂ = 0.2194 (6295)
Temperature(K)	150 K	294 K
CCDC	2363480	2050015

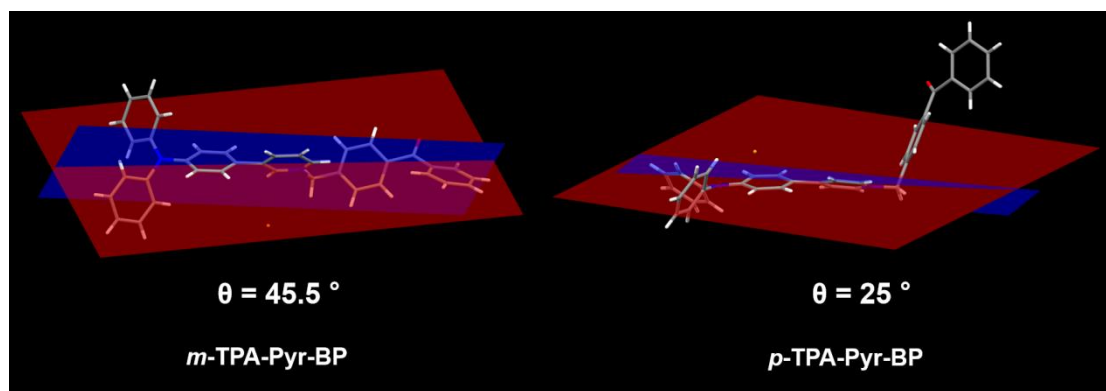


Figure. S8 The torsion angel (θ) between the benzene ring in triphenylamine and the adjacent pyridine of *m*-TPA-Pyr-BP and *p*-TPA-Pyr-BP under their single crystal.

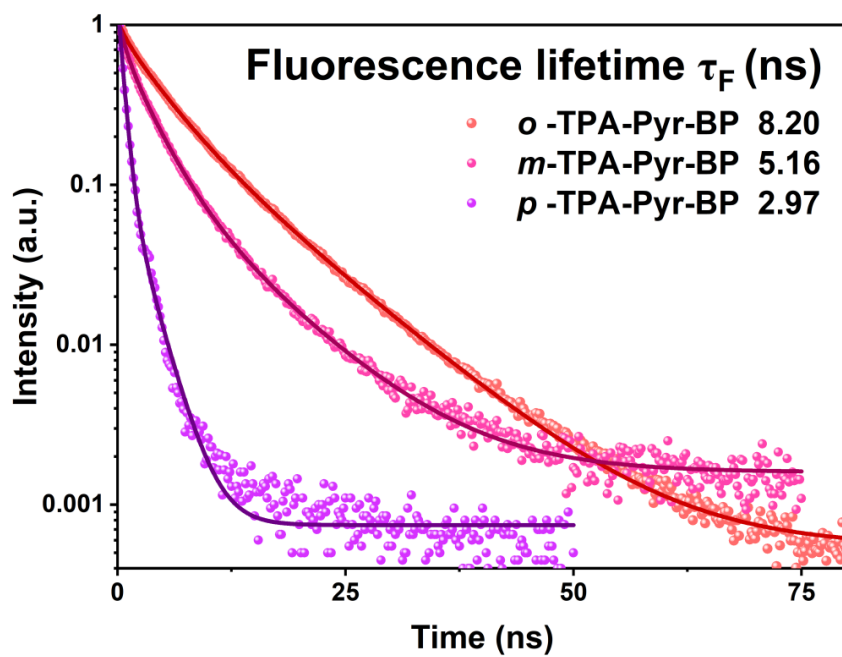


Figure. S9 Lifetime decay profiles of *o*-, *m*-, *p*-TPA-Pyr-BP in solid powders.

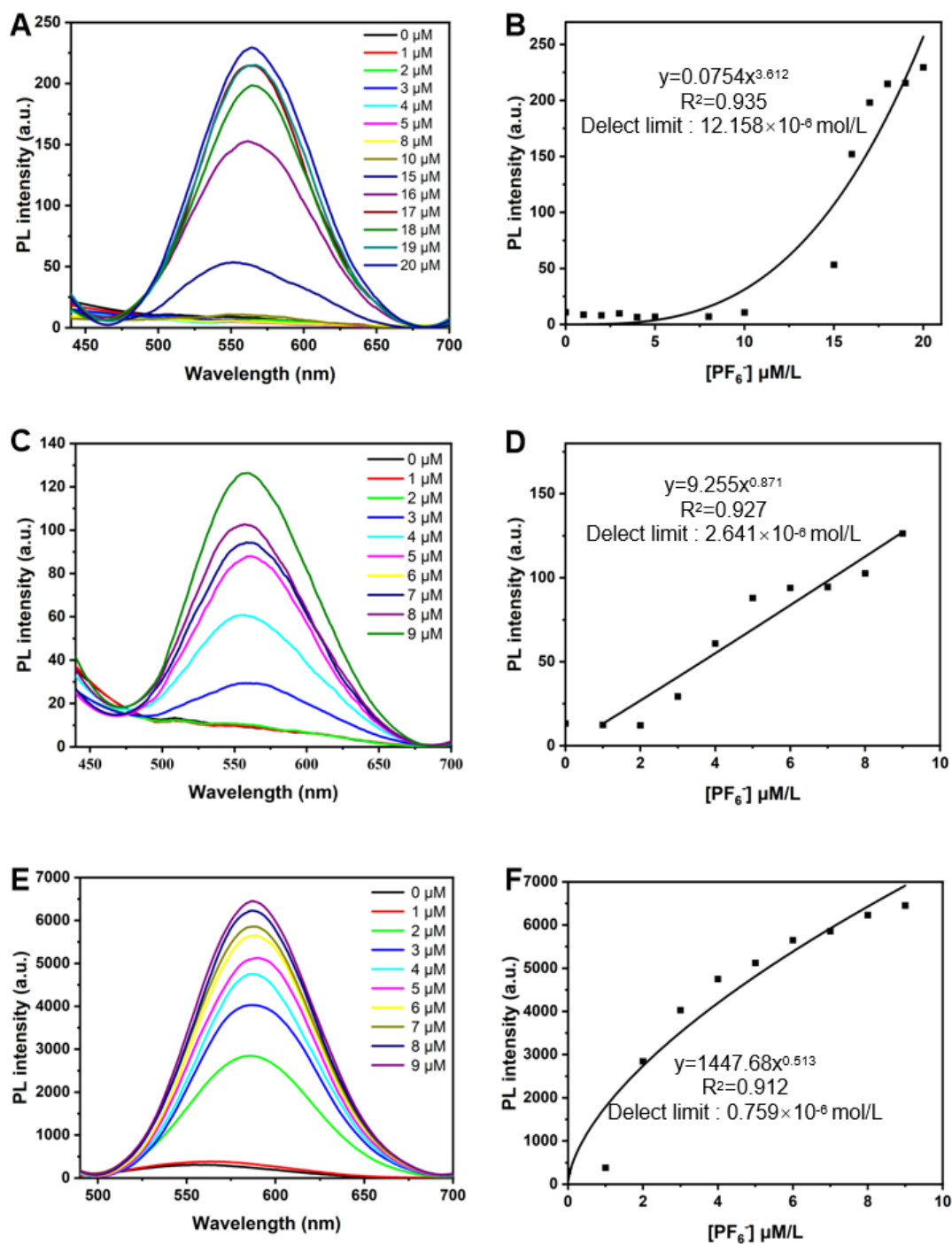


Figure. S10 Plot of fluorescence intensity change of *o*-TPA-Pyr-BP (A), *m*-TPA-Pyr-BP (C), *p*-TPA-Pyr-BP (E) with various concentrations of PF₆⁻ at 25 °C; The limit detection of *o*-TPA-Pyr-BP (B), *m*-TPA-Pyr-BP (D), *p*-TPA-Pyr-BP (F) were calculated by the formula (3σ/K) (Conc. = 10 μM, λ_{ex} = 420, 400 and 460 nm, respectively.)

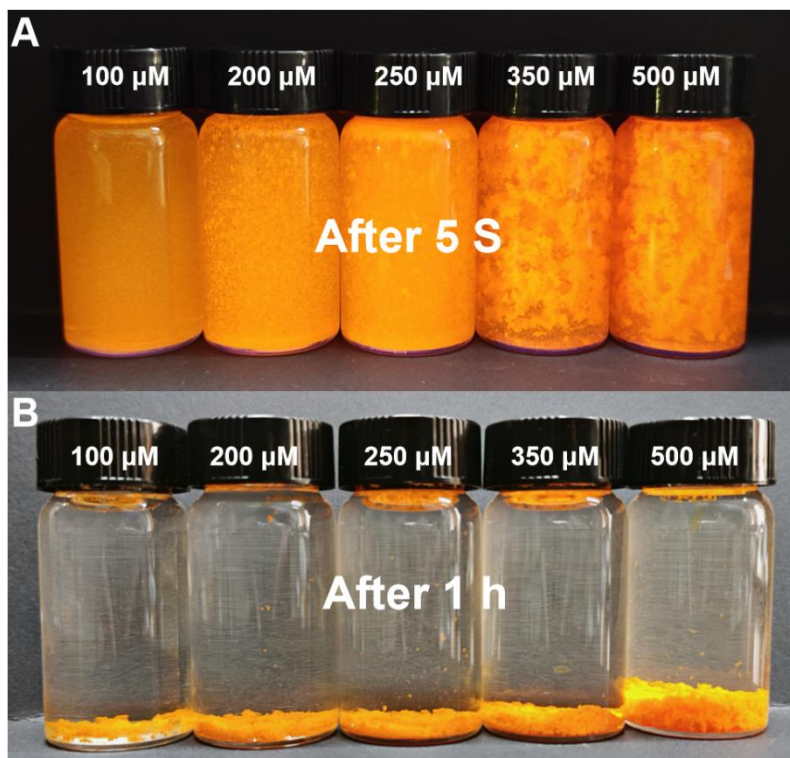


Figure. S11 Sensing photographs of adding equal equivalents of PF_6^- to different concentrations of *p*-TPA-Pyr-BP (methanol: water = 1: 9, 20 mL); above: After adding PF_6^- to the solution for 5 seconds (**A**); bottom: After adding PF_6^- to the solution for 1 hour (**B**).

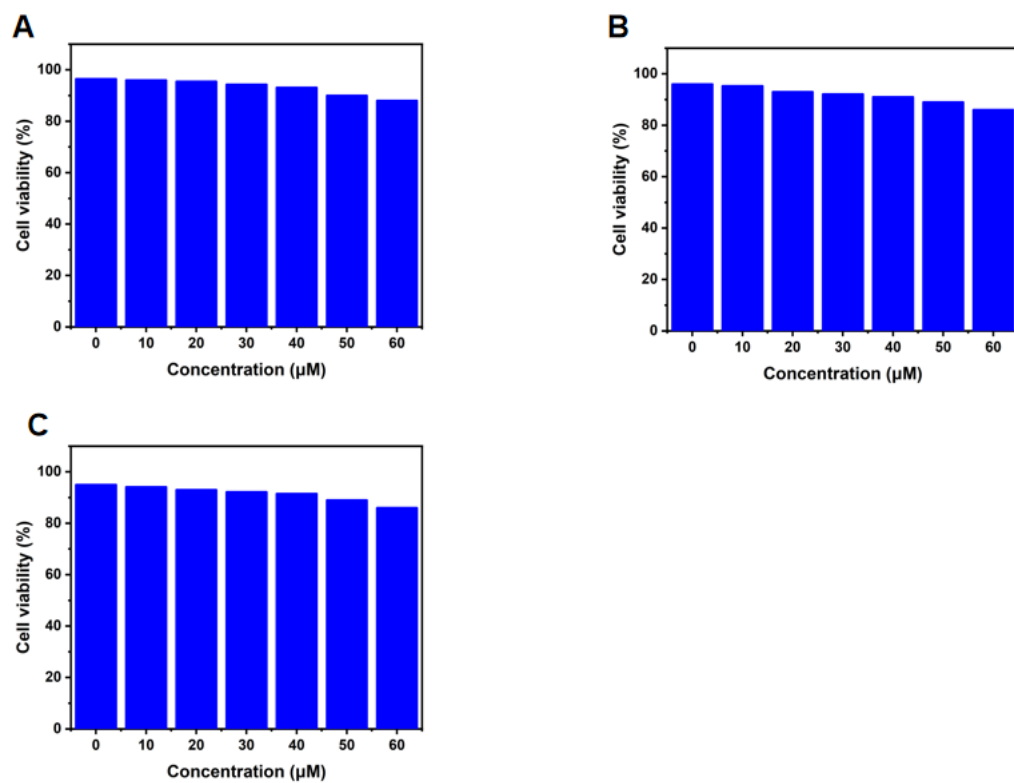


Figure. S12 HeLa cells viability assessed by MTT assay of *o*-TPA-Pyr-BP (**A**), *m*-TPA-Pyr-BP (**B**), *p*-TPA-Pyr-BP (**C**) in various concentrations at 37 °C for 24 hours.

3. NMR data spectra

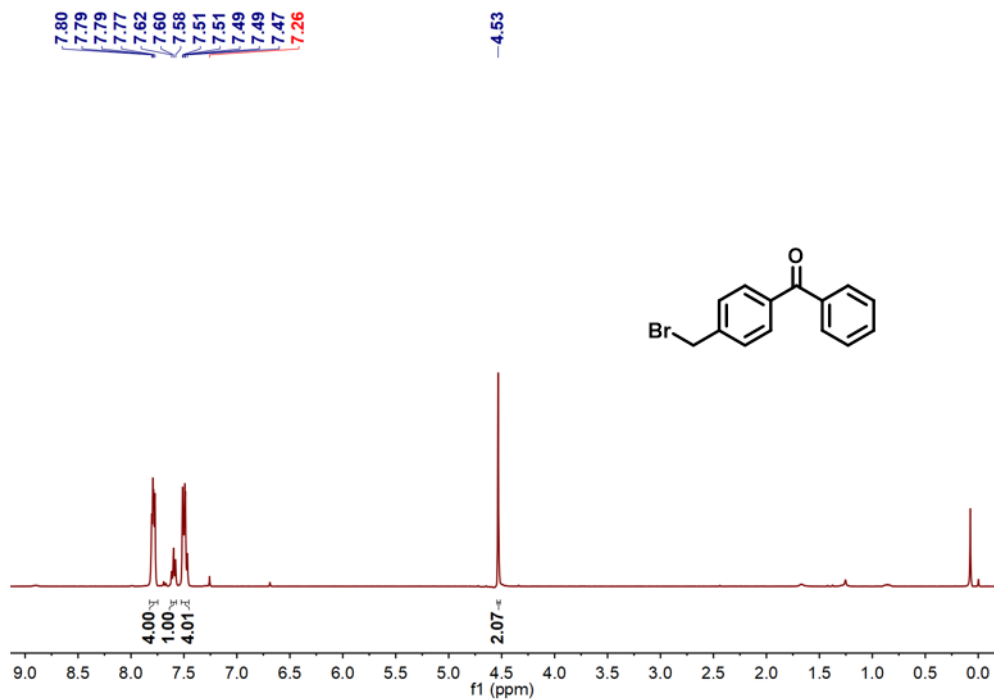


Figure. S13 ^1H NMR spectra of BP-Me-Br in CDCl_3 .

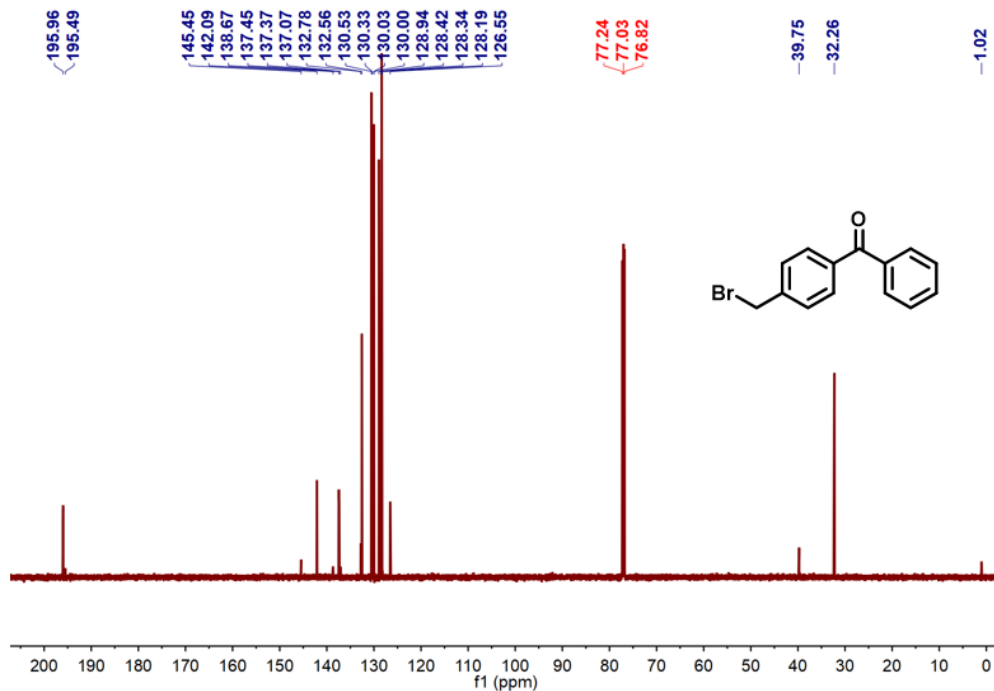


Figure. S14 ^{13}C NMR spectra of BP-Me-Br in CDCl_3 .

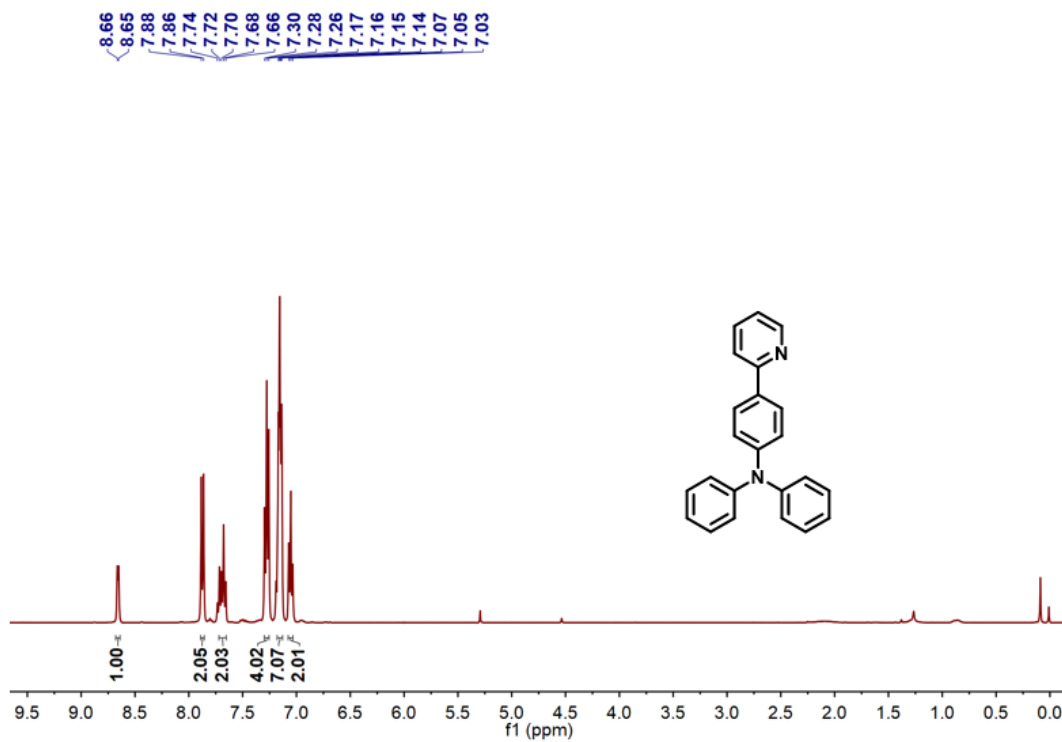


Figure. S15 ^1H NMR spectra of *o*-TPA-Py in CDCl_3 .

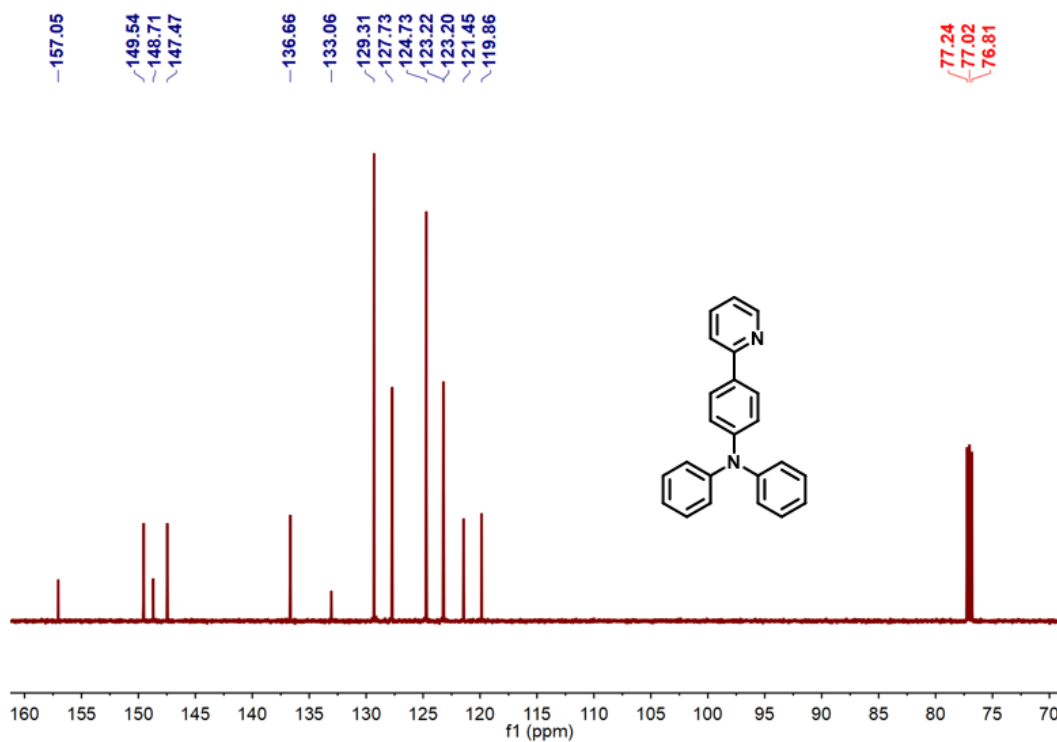


Figure. S16 ^{13}C NMR spectra of *o*-TPA-Py in CDCl_3 .

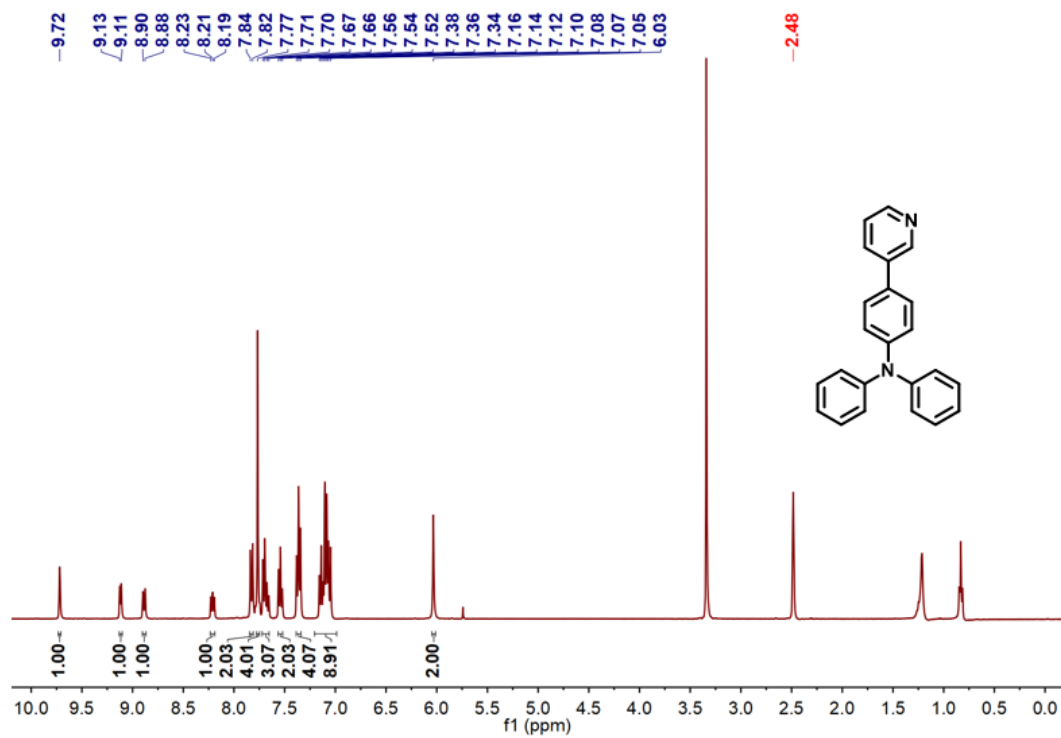


Figure. S17 ^1H NMR spectra of *m*-TPA-Py in $\text{DMSO-}d_6$.

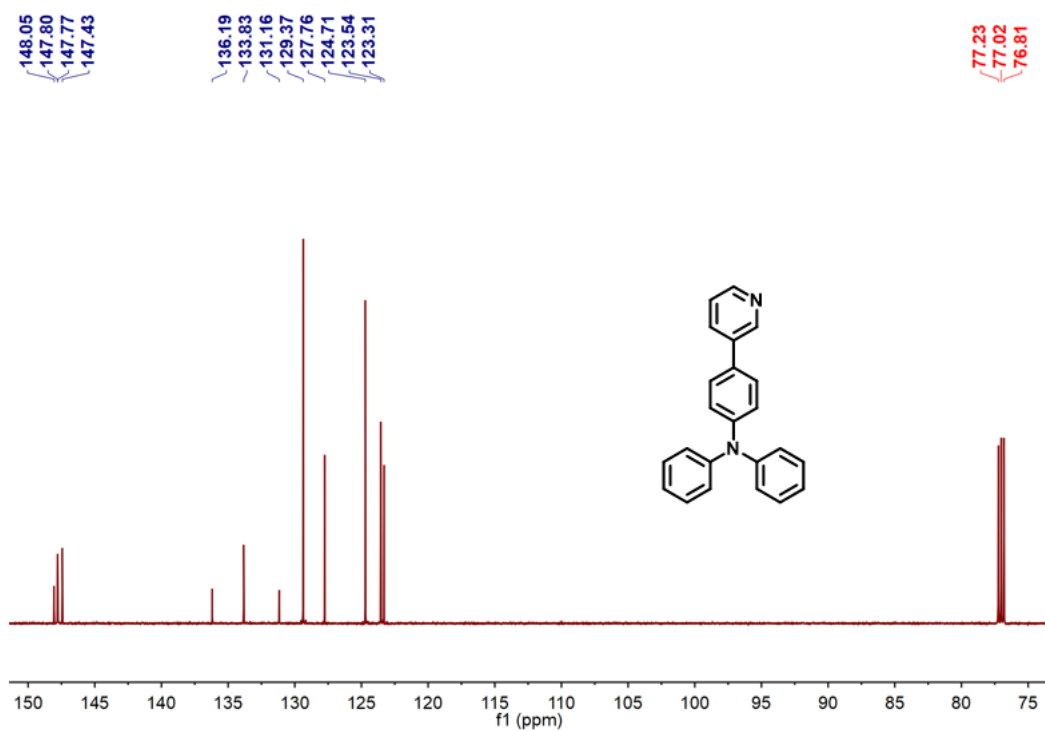


Figure. S18 ^{13}C NMR spectra of *m*-TPA-Py in CDCl_3 .

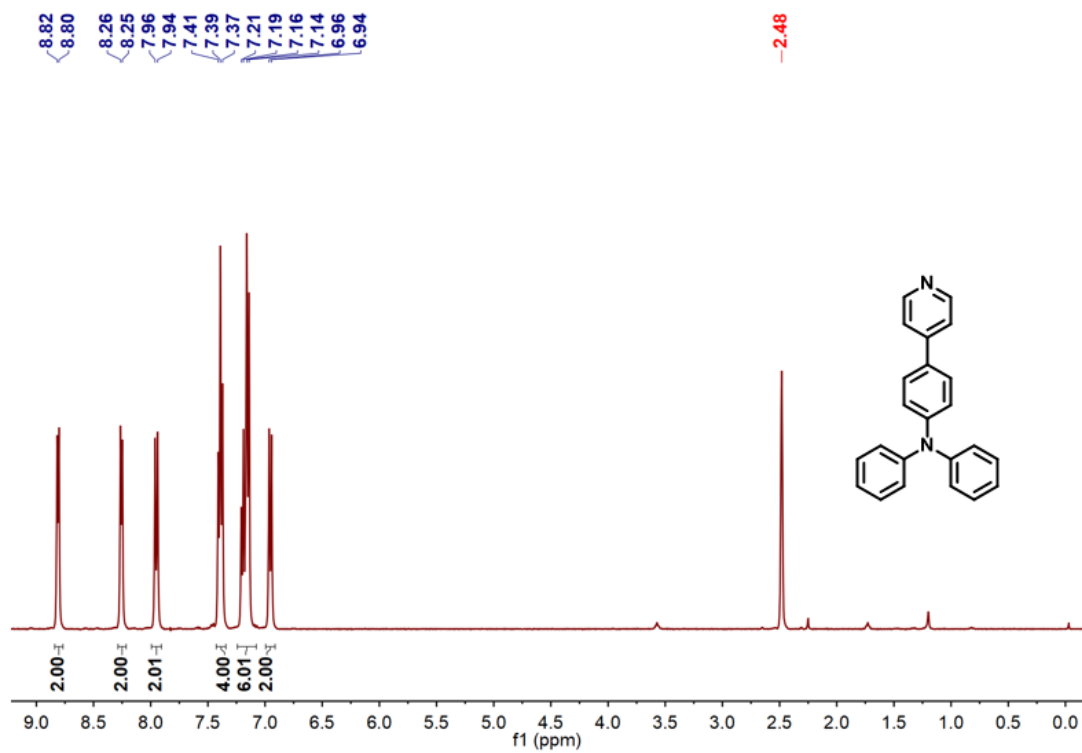


Figure. S19 ^1H NMR spectra of *p*-TPA-Py in $\text{DMSO-}d_6$.

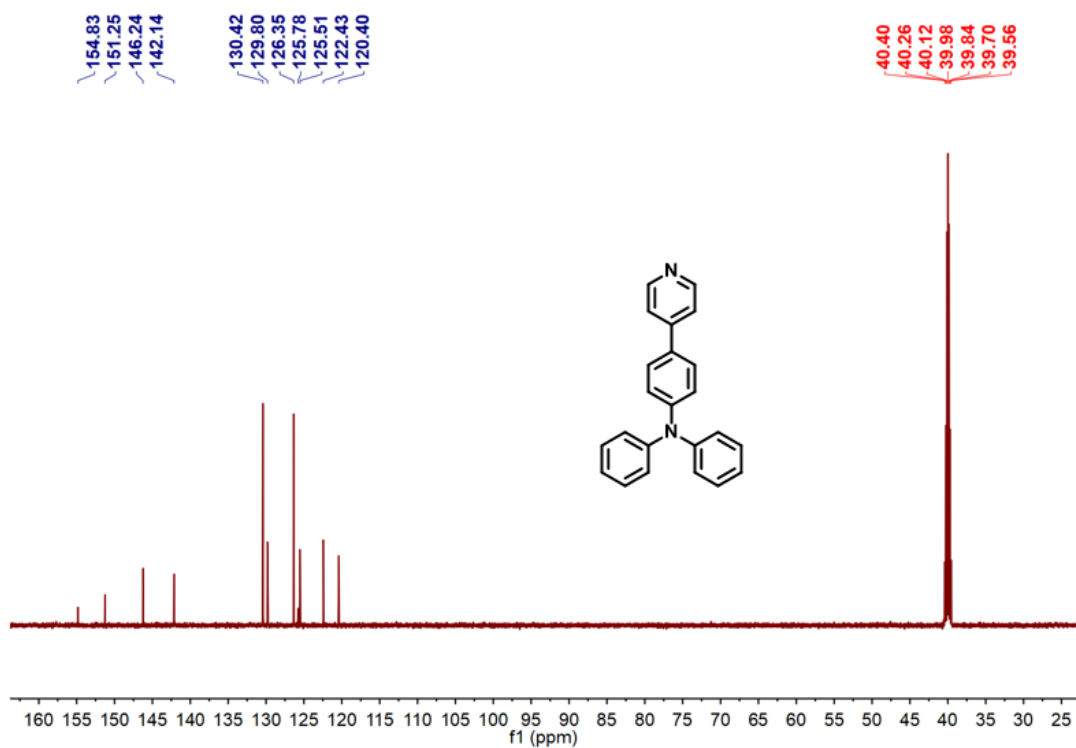


Figure. S20 ^{13}C NMR spectra of *p*-TPA-Py in $\text{DMSO-}d_6$.

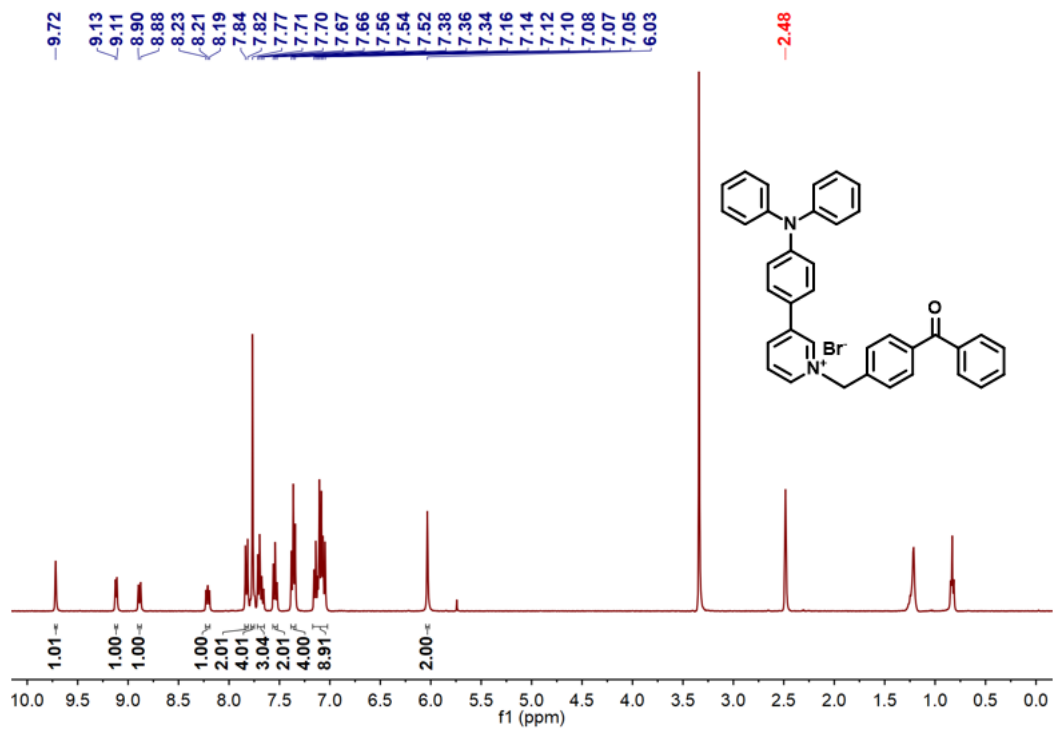


Figure. S23 ^1H NMR spectra of *m*-TPA-Pyr-BP in $\text{DMSO-}d_6$.

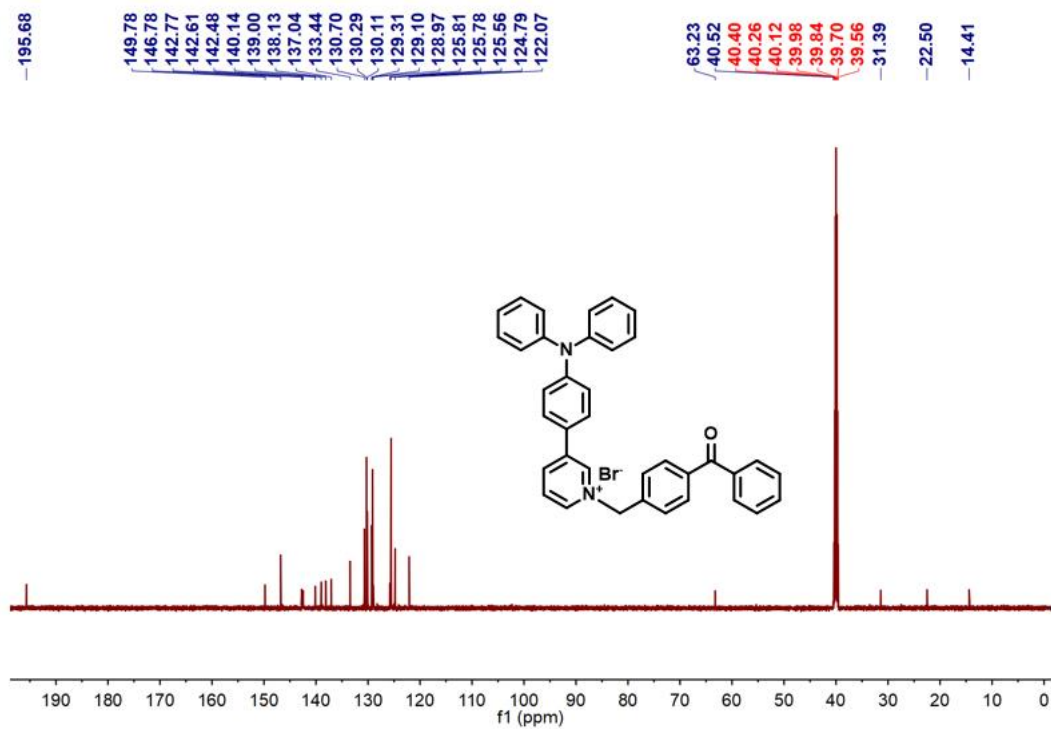


Figure. S24 ^{13}C NMR spectra of *m*-TPA-Pyr-BP in $\text{DMSO-}d_6$.

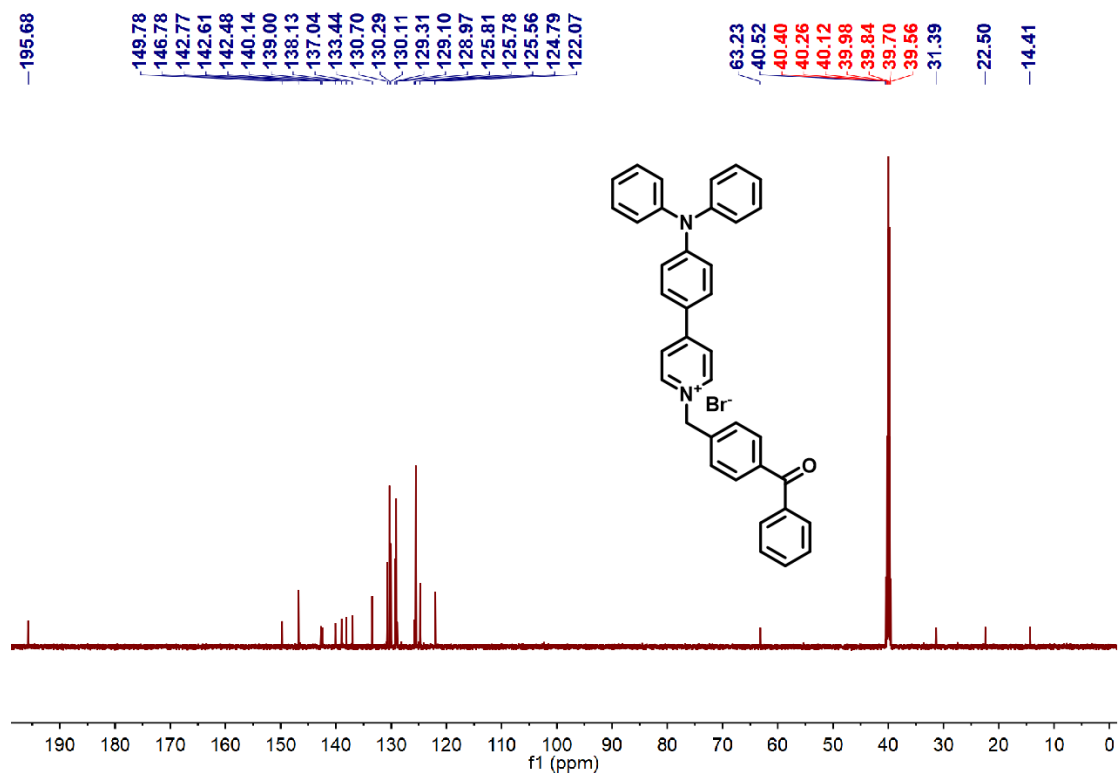


Figure. S25 ¹³C NMR spectra of *p*-TPA-Pyr-BP in DMSO-*d*₆.

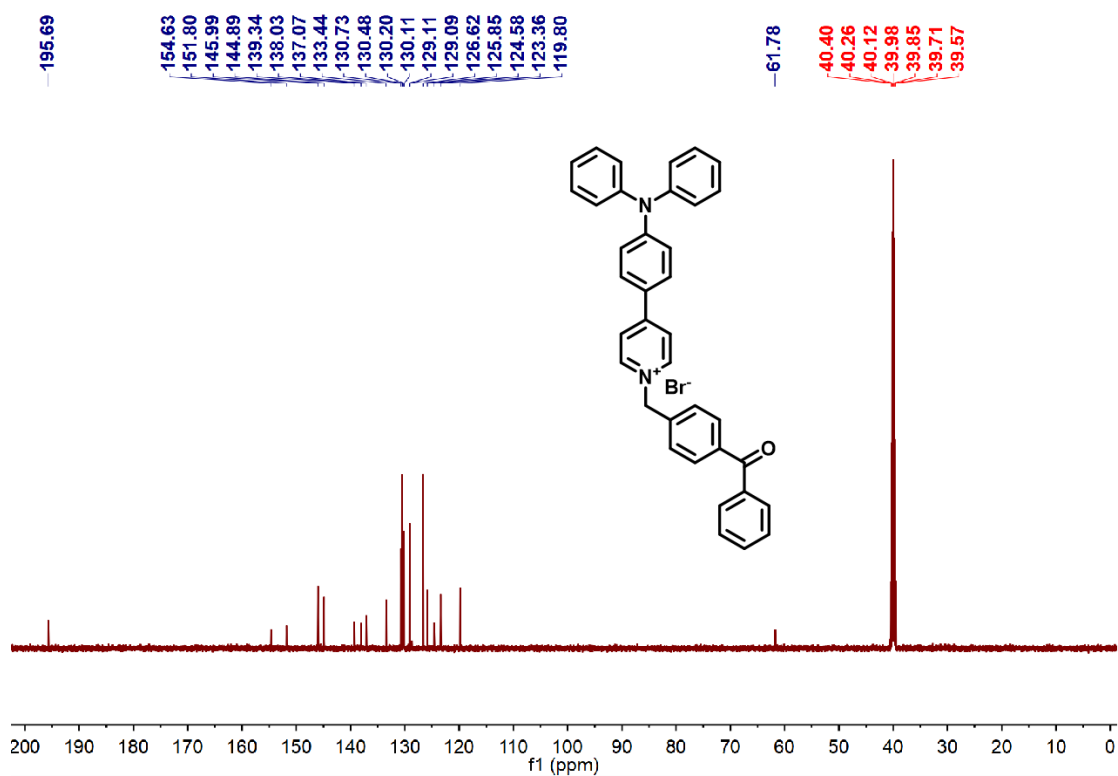


Figure. S26 ¹³C NMR spectra of *p*-TPA-Pyr-BP in DMSO-*d*₆.

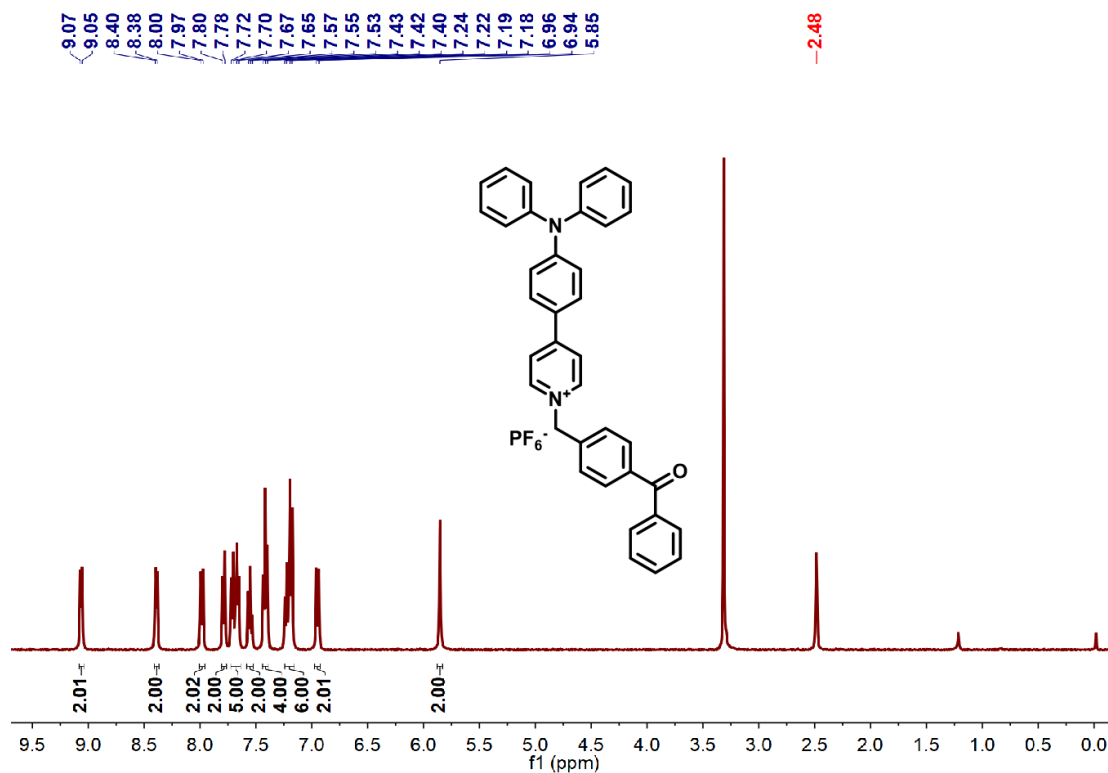


Figure. S27 ¹H NMR spectra of *p*-TPA-Pyr-BP (PF₆⁻) in DMSO-*d*₆.

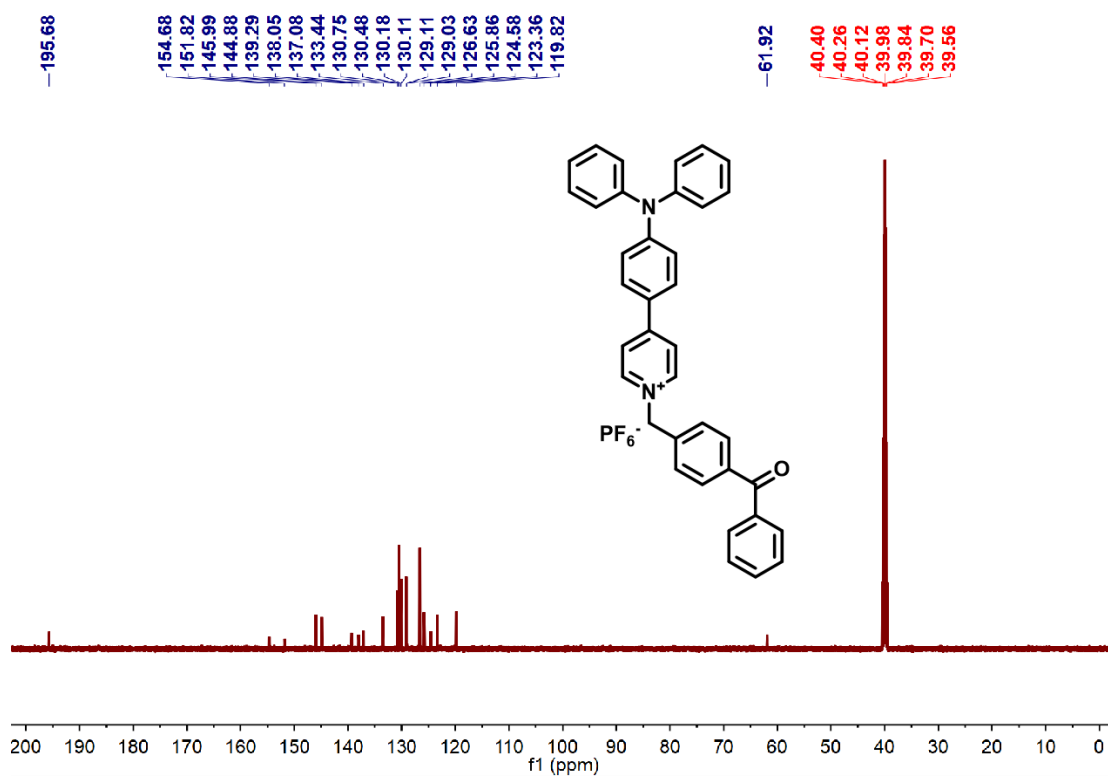


Figure. S28 ¹³C NMR spectra of *m*-TPA-Pyr-BP (PF₆⁻) in DMSO-*d*₆.

4. HRMS date spectra

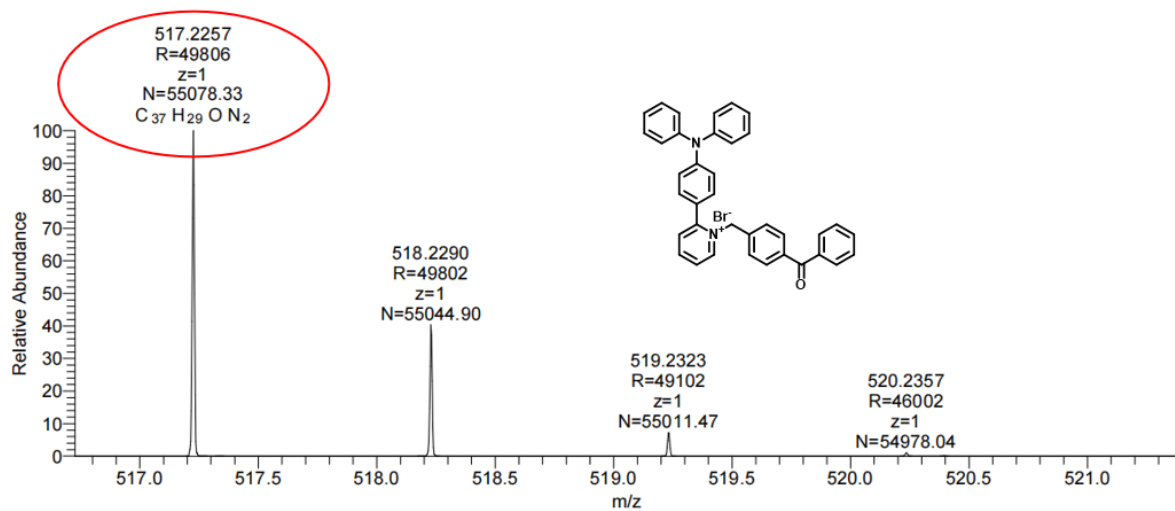


Figure. S29 HRMS spectra of *o*-TPA-Pyr-BP.

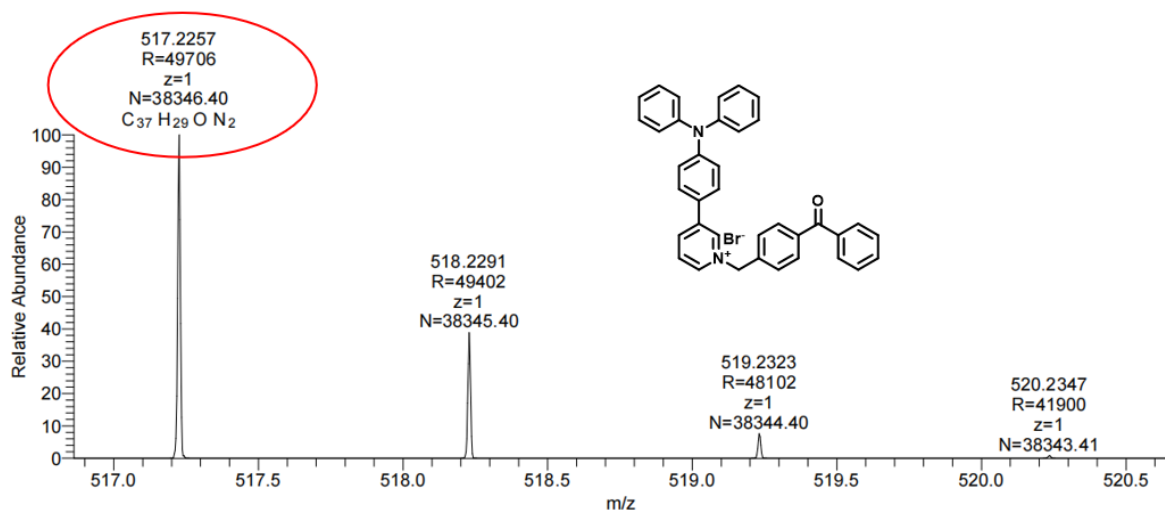


Figure. S30 HRMS spectra of *m*-TPA-Pyr-BP.

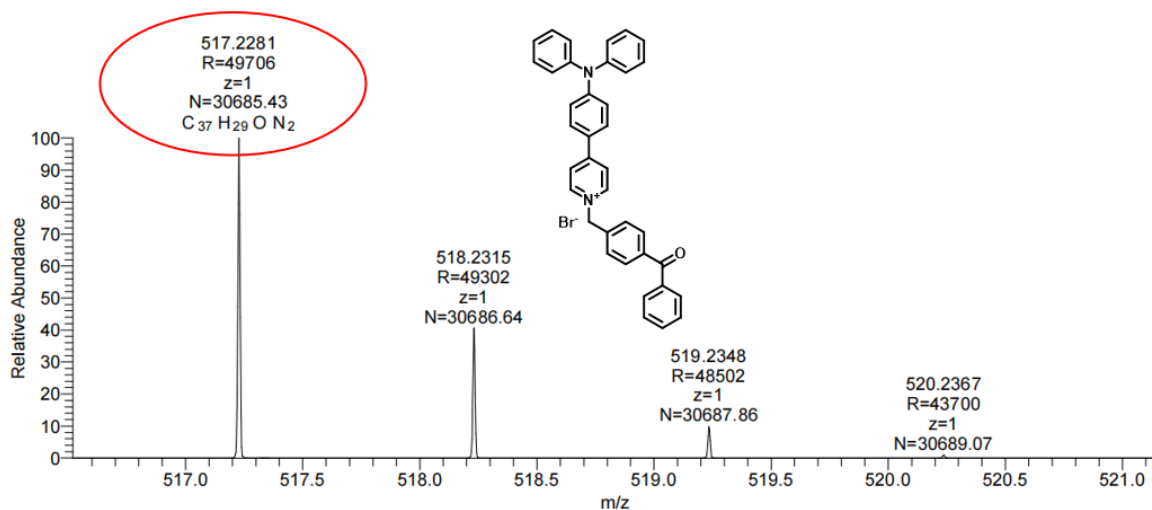


Figure. S31 HRMS spectra of *p*-TPA-Pyr-BP.

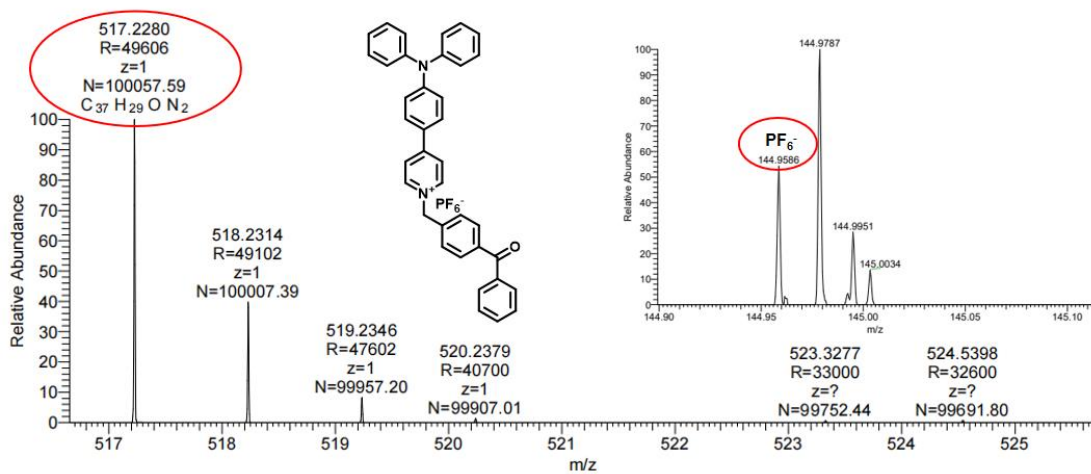


Figure. S32 HRMS spectra of *p*-TPA-Pyr-BP/PF₆⁻.

5. REFERENCES

- [1] Liu, R. Y.; Zhang, P. W.; Gan, Tong, Cook, James M. Regiospecific Bromination of 3-Methylindoles with NBS and Its Application to the Concise Synthesis of Optically Active Unusual Tryptophans Present in Marine Cyclic Peptides. *J. Org. Chem.*, 1997, **62**, 7447-7456.
- [2] Yin, W. D.; Yang, Z. M.; Yang, Y.; Li, X. X.; Li, Z.; Zhang, B.; Zhang, S. J.; Han, B. Y.; Ma, H. C. A positively charged aggregation-induced emission (AIE) luminogen as an ultra-sensitive mechanochromic luminescent material: design, synthesis and versatile applications. *Mater. Chem. Front.*, 2021, **5**, 2849.
- [3] Ma, H. C.; Yang, Z. M.; Cao, H. Y.; Lei, L.; Chang, L.; Ma, Y. C.; Yang, M. Y.; Yao, X. Q.; Sun, S. B.; Lei, Z. Q. One bioprobe: a fluorescent and AIE-active macromolecule; two targets: nucleolus and mitochondria with long term tracking. *J. Mater. Chem. B*, 2017, **5**, 655-660.
- [4] Zhou, X.; Wang, X. H.; Zhang, T. Y.; Shen, L. Y.; Yang, X. J.; Zhang, Q. L.; Xu, H.; Redshaw, C.; Xing, F. Pyrene-Based Cationic Fluorophores with High Affinity for BF_4^- , PF_6^- , and ClO_4^- Anions: Detection and Removal. *J. Org. Chem.*, 2023, **88**, 13520-13527.